Title	Dual-band monopole antenna with frequency-tunable feature for WiMAX applications
Author(s)	Sun, X; Cheung, SW; Yuk, TTI
Citation	IEEE Antennas and Wireless Propagation Letters, 2013, v. 12, p. 100-103
Issued Date	2013
URL	http://hdl.handle.net/10722/189079
Rights	IEEE Antennas and Wireless Propagation Letters. Copyright © Institute of Electrical and Electronics Engineers.

Dual-Band Monopole Antenna With Frequency-Tunable Feature for WiMAX Applications

X. L. Sun, S. W. Cheung, *Senior Member, IEEE*, and T. I. Yuk, *Member, IEEE*

***Abstract*—A planar dual-band monopole antenna with a frequency-tunable band is presented. The structure of the antenna radiator has a stem connecting to two branches that are used to generate two frequency bands at around 2.4 and 3.4 GHz for Worldwide Interoperability for Microwave Access (WiMAX) applications. The lower band covers the WiMAX frequency band of 2.3–2.4 GHz, while the higher band is frequency-tunable to the WiMAX frequency bands of 3.3–3.4, 3.4–3.6and 3.6–3.8 GHz. The frequency tunability is achieved by using the reverse-bias voltage across a varactor that is placed between the stem and one of the radiating branches of the radiator. In this study, the radiating branch responsible for the higher band is selected for tuning. A simple and novel biasing circuit, consisting of two radio frequency (RF) choke resistors and an L-shaped stub, is designed for biasing the varactor. Results show that the higher band can be continuously tuned in frequency, yet keeping the lower band unchanged. The reflection coefficient, radiation pattern, and efficiency of the antenna are studied using computer simulation and measurement.**

***Index Terms*—Biasing circuit, dual-band, frequency-tunable, WiMAX.**

I. Introduction

THE DEMAND for integrating multiple wireless standards into a single wireless platform is increasing, and fixed multiband antennas are lacking the flexibility to accommodate new services [1], so the design of reconfigurable antennas is getting momentum [2]–[9]. Frequency-reconfigurable antennas can be classified into two categories, namely *band switching* and *continuous tuning*. Band switching can be achieved using p-i-n diode switches, and the operating frequency band is switched among different frequency bands, depending on the switching states [2]–[4], [9]. Continuous tuning can be accomplished using varactor diodes, and the antennas can be frequency-tuned smoothly within or between operating bands [5]–[8]. In these antennas, direct current (dc) biasing circuits are needed to operate the p-i-n or varactor diodes. In the design of reconfigurable antennas using patch or planar inverted-F antennas (PIFAs), the biasing circuit is quite simple and straightforward [2]–[8]. The patch antenna, occupying larger area and with directional radiation pattern, is not the best choice for wireless devices. As users are looking for thinner wireless devices, the PIFA with high profile is becoming less attractive. The planar monopole antenna, having simple structure and omnidirectional radiation, is becoming more popular. The monopole antenna is usually wideband, but the reconfigurable antenna based on using narrowband monopole can be made more selective to reject more out-of-band noise. However, since there is no ground underneath the radiator of monopole antennas, using the biasing circuits in [2]–[8] would increase the circuit complexity and interference with the antenna. To the best knowledge of the authors, there has been very little work on frequency tuning of monopole antennas using varactor or p-i-n diodes located on the radiator. One study on a frequency-reconfigurable multiple-input–multiple-output (MIMO) antenna using monopole radiators was found in [9], where a piece of wire was used to feed the dc power to the p-i-n diode with a radio frequency (RF) choke inductor to isolate the wire from the radiator. A Bias T was used at the antenna input to provide a dc ground. In such a design, the wire used in the biasing circuit would cause inconveniences in prototyping or manufacturing the antenna.

In this letter, a planar dual-band monopole antenna having a frequency-tunable higher band is presented. The radiator of the antenna consists of a short stem connecting to two branches to generate two frequency bands at around 2.4 and 3.4 GHz for WiMAX applications. The tunability of the frequency band is achieved by placing a varactor between the relevant branch and the short stem of the radiator. Varying the reveres-bias voltage of the varactor will vary the varactor capacitance, which in turn will vary the resonance of the antenna. With the varactor placed on the radiator, the biasing circuit for the varactor will be quite sensitive to the antenna performance and so must be carefully designed to reduce the effects. Here, a novel biasing circuit, which is free of any soldering wire on the antenna, is proposed. The antenna with the biasing circuit is studied using the electromagnetic (EM) simulation tool CST. For verification of simulation results, the antenna is also fabricated and measured using the antenna measurement system Satimo Starlab.

II. Antenna Design

The geometry of the proposed frequency-tunable antenna is shown in Fig. 1. It is a planar dual-band monopole antenna that is microstrip-fed. The radiator has a short stem and two branches. Branch 1 is folded, and branch 2 is meandered to achieve a compact size. They are designed to resonate at around

Manuscript received December 26, 2012; accepted January 17, 2013. Date of publication January 23, 2013; date of current version March 12, 2013.

The authors are with the Department of Electrical and Electronic Engineering, The University of Hong Kong, Hong Kong (e-mail: xlsun@eee.hku.hk; swcheung@eee.hku.hk; tiyuk@eee.hku.hk).

Color versions of one or more of the figures in this letter are available online at http://ieeexplore.ieee.org.

Digital Object Identifier 10.1109/LAWP.2013.2242252

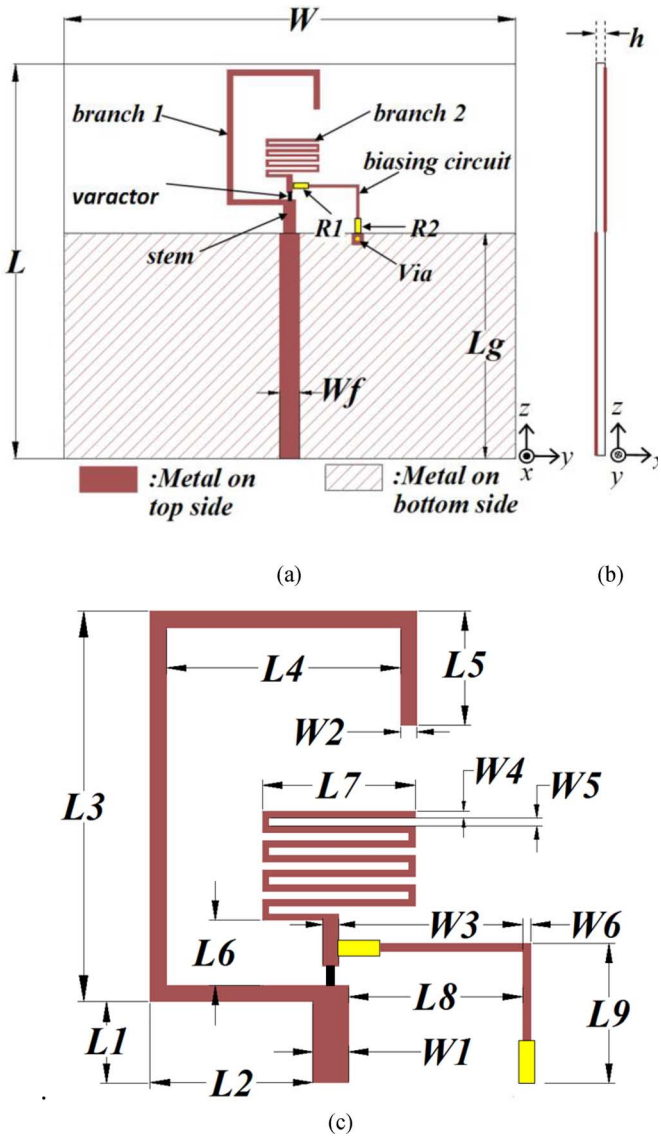

Fig. 1. Geometry of antenna: (a) front view, (b) side view, and (c) radiator.

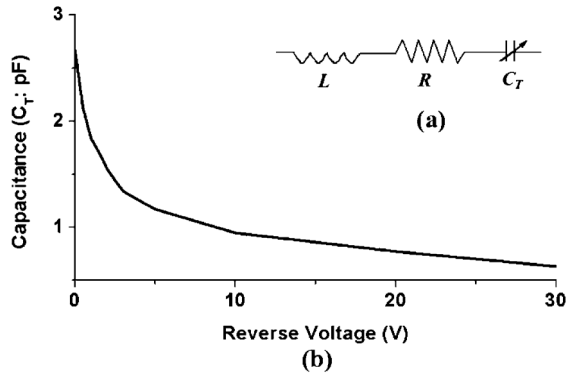

Fig. 2. (a) Simulation model for varactor and (b) capacitance C_T versus dc bias voltage for varactor SMV1405 (obtained from datasheet).

TABLE I
OPTIMIZED DIMENSIONS OF ANTENNA (MILLIMETERS)

W	*40*	*L1*	*2.5*	*L6*	*2*	*W2*	*0.5*
L	*35*	*L2*	*5*	*L7*	*4.7*	*W3*	*0.5*
Wf	*1.8*	*L3*	*12*	*L8*	*5.35*	*W4*	*0.2*
Lg	*20*	*L4*	*7.2*	*L9*	*4.3*	*W5*	*0.25*
h	*0.8*	*L5*	*3.5*	*W1*	*1.1*	*W6*	*0.25*

2.4 and 3.4 GHz. The antenna is designed on a $(W \times L \times h =)$ $40 \times 35 \times 0.8$-mm^3 Rogers substrate, 4350B, with a relative permittivity of 3.5 and a loss tangent of 0.004. To enable tunability of the higher band at 3.4 GHz, a varactor is placed between branch 2 and the stem of the radiator. In our design, we use a practical varactor SMV 1405-79 from Skyworks, with a physical dimension of $1.2 \times 0.7 \times 0.5$ mm^2. In computer simulation, the varactor is modeled using a simple circuit as shown in Fig. 2(a), where the parasitic inductance $L = 0.7$ nH and the parasitic resistor $R = 0.8\ \Omega$ are obtained from the datasheet. The capacitance C_T varies from 2.67 to 0.63 pF for the bias voltage from 0 to 30 V, as shown in Fig. 2(b).

Since the varactor is placed in series with branch 2 and the stem of the radiator, the biasing circuit needs to be carefully designed to avoid serious effects on the antenna performance. Here, we propose a simple and novel biasing circuit for the varactor. To provide a dc path for the varactor, a narrow L-shaped stub is printed on the same side of the radiator, as shown in Fig. 1(a) or (c). One end of the stub is connected to branch 2 using resistor $R1$, and the other end is connected to another resistor $R2$ and then a via to the ground. The two resistors have a dimension of $2 \times 1.2 \times 0.5$ mm^3 and value of 2.3 kΩ, which are used as RF chokes to prevent the RF signal from getting into the L-shaped stub. The L-shaped stub and the two resistors form a dc loop from the feedline to the antenna ground. This makes the biasing very simple because the ground is now common to both the RF and dc signals. The bias dc voltage for the varactor can simply be added to the RF signal and then fed to the microstrip feedline. One main advantage of the proposed biasing technique is that no additional wire is needed to be soldered on the antenna. (Note that we can use the same technique to tune the lower band. However, we cannot use the technique to tune both higher and lower bands independently and simultaneously because, at any one time, we can only apply one bias dc voltage to the feed line.) The antenna with the biasing circuit is studied and optimized using the EM simulation tool CST. The optimized dimensions are listed in Table I and used to fabricate the antenna.

III. SIMULATION AND MEASUREMENT RESULTS

Computer simulation has been used to study the effects of the biasing circuit on the frequency bands of the antenna. The simulated S_{11} of the antenna using a bias voltage of 0 V (equivalent to $C_T = 2.67$ pF in the varactor) and without using the biasing circuit are shown in Fig. 3. It can be seen that the proposed biasing circuit has very little effect on the S_{11} of the antenna.

The tunability of the antenna is studied with the bias voltages of 0, 4, and 24 V in the varactor. In simulation, these voltages are represented using the corresponding values of $C_T = 2.67$, 1.25, and 0.7 pF in the varactor model of Fig. 2(a). No feeding cable is needed in simulation. In actual measurement, the bias voltages are obtained from a dc power supply and added to the RF signal

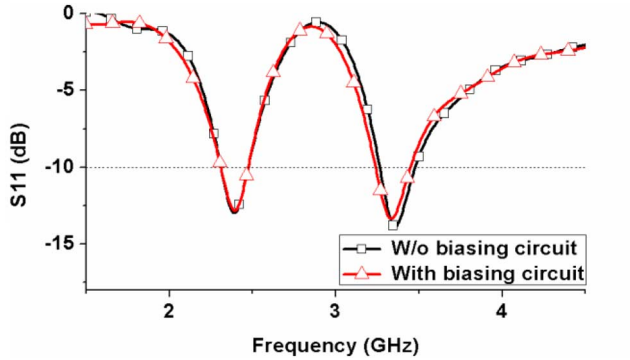

Fig. 3. Simulated S_{11} with and without biasing circuit.

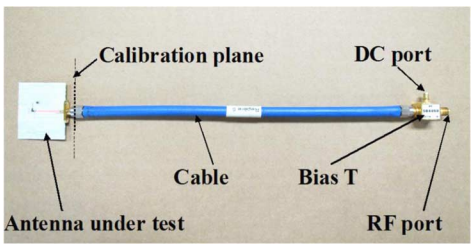

Fig. 4. Prototyped antenna with short feeding cable and Bias T.

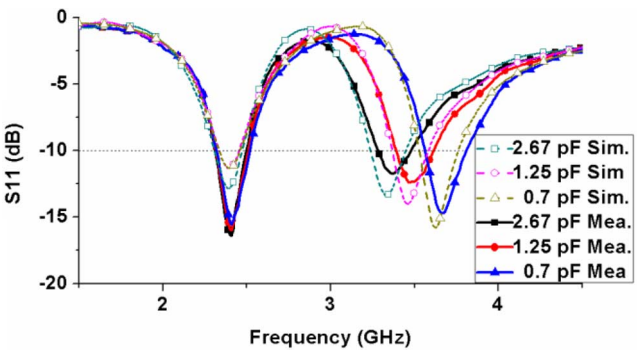

Fig. 5. Simulated and measured S_{11} with $C_T = 2.67,\ 1.25$ and 0.7 pF.

using a Bias T. Moreover, a short feeding cable (a 22-cm-long coaxial cable), as shown in Fig. 4, provided by Satimo is used to connect the antenna to the system. To reduce the effects of the Bias T on the measured radiation pattern (as will be explained later), the combined signal from the Bias T is fed to the feeding cable and then to the antenna. Calibration is performed before actual measurement, so the measurement is referenced to the calibration plane (including the SMA connector), as shown in Fig. 4. This eliminates the insertion losses caused by the cable and the Bias T, etc., in the measured results.

The simulated and measured S_{11} of the antenna are shown in Fig. 5. It can be seen that the simulated and measured resonant frequencies agree very well. The discrepancies are mainly due to the: 1) effects of the feeding cable used in measurement; 2) accuracy of the simulation model for the varactor; 3) use of an ideal model for the resistors in simulation; 4) fabrication tolerances in antenna; and 5) measurement tolerance. With $C_T = 2.67$ pF, the lower and higher bands are at 2.4 and 3.37 GHz, respectively. With C_T decreased to 1.25 and 0.7 pF, the measured resonance in the higher band shifts to 3.47 and

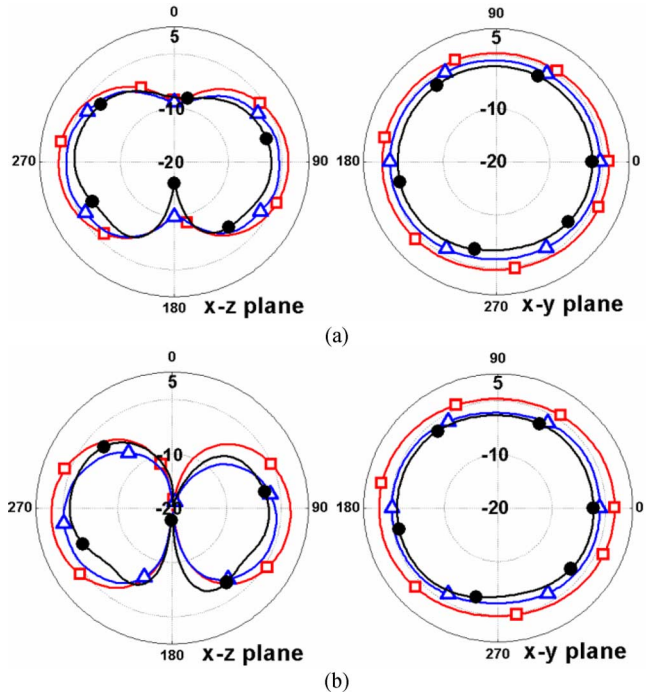

Fig. 6. Simulated and measured radiation patterns in xz- and xy-planes at (a) 2.4 and (b) 3.4 GHz. (—□—: Sim. without cable. —△—: Sim. with cable. —●—: Mea.).

3.67 GHz, respectively, achieving a tuning range of 300 MHz. The measured bandwidths ($S_{11} < -10$ dB) at these three higher resonant frequencies are 190 MHz (3.28–3.47GHz), 220 MHz (3.39–3.61 GHz), and 250 MHz (3.56–3.81 GHz). Note that the resonant frequency of the lower band remained unchanged at 2.4 GHz (2.3–2.5 GHz) while tuning the higher frequency band.

The radiation patterns of the antenna with and without using the biasing circuit have also been studied using simulation and measurement. Both results have indicated that the biasing circuit has insignificant effect on the radiation patterns. Moreover, the antenna has similar radiation patterns at different resonant frequencies in the higher band. Thus, we only present the results at the lower frequency of 2.4 GHz and higher frequency of 3.4 GHz (with $C_T = 2.67$) in Fig. 6.

In measurement, a feeding cable as shown in Fig. 4 is always needed to connect the antenna to the measurement system. When measuring small monopoles at low frequencies where the finite grounds become electrically small, some currents will flow back to the outer surface of the feeding cable, causing secondary radiation from the cable [10], [11] and inaccuracies to the measured radiation patterns. Thus, to produce more accurate results on radiation pattern measurement, the feeding cable provided by Satimo for use with the Starlab system is covered with EM suppressant tubing to absorb the secondary radiation. With this approach, the measured gain and efficiency of the antenna will be lower than the actual values because some radiated power is absorbed by the EM suppressant tubing and does not get measured by the measurement system. Since the Bias T used is not covered with EM suppressant material and so will affect the results on radiation pattern measurement, we place it at the other end of the short feeding cable (farther away from

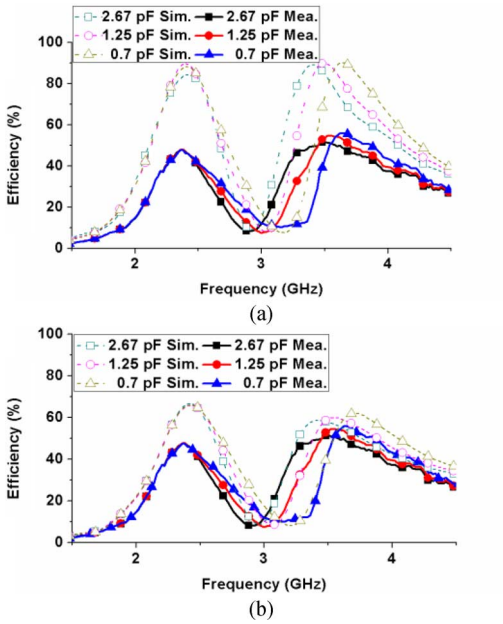

Fig. 7. (a) Simulated efficiencies without cable model and measurement efficiencies. (b) Simulated efficiencies with cable model and measured efficiencies, with $C_T = 2.67$, 1.25, and 0.7 pF.

the antenna) to reduce its effects. To illustrate the cable effects on the measured results, the antenna together with the feeding cable is modeled in CST as we did in [11]. For comparison, the simulation radiation patterns with the cable model are also shown in Fig. 6. It can be seen that the antenna behaves like a monopole antenna. The simulated radiation patterns without using the cable have larger discrepancies with the measured results due to cable effects. When the cable model is used, the simulated gains at all directions decrease and have a better agreement with the measurement. The small discrepancies are mainly due to the parameters used to model the EM suppressant tubing not being precisely accurate.

Fig. 7 shows the simulated efficiencies with and without using the cable model at different bias voltages and also the corresponding measured efficiencies for comparison. It can be seen that the measured efficiencies are all very much less than those of the simulated results without the cable model. This is again due to the EM suppressant tubing on the feeding cable, as described previously. With using the cable model, the simulated and measured results have much better agreements. Fig. 7 shows that, with $C_T = 2.67$, 1.25, and 0.7 pF, the efficiencies in both the lower band and higher band remain relatively constant.

IV. Conclusion

A dual-band monopole antenna with a frequency-tunable higher band has been presented. A varactor is used the radiator for tuning the frequency band. A simple and novel biasing circuit has been proposed to bias the varactor. Results have shown that the biasing circuit has little effects on the antenna performance. The higher band of the antenna can be tuned continuously between 3.37–3.67 GHz, yet the lower band at around 2.4 GHz remains unchanged. Good radiation patterns are achieved in the working bands.

References

[1] S. Yang, C. Zhang, H. Pan, A. Fathy, and V. Nair, "Frequency reconfigurable antennas for multiradio wireless platforms," *IEEE Microw. Mag.*, vol. 10, no. 1, pp. 66–83, Feb. 2009.

[2] H. F. AbuTarboush, R. Nilavalan, S. W. Cheung, K. M. Nasr, T. Peter, and D. Budimir, "A reconfigurable wideband and multiband antenna using dual-patch elements for compact wireless devices," *IEEE Trans. Antennas Propag.*, vol. 60, no. 1, pp. 36–43, Jan. 2012.

[3] A. F. Sheta and S. F. Mahmoud, "A widely tunable compact patch antenna," *IEEE Antennas Wireless Propag. Lett.*, vol. 7, pp. 40–42, 2008.

[4] T. Y. Han and C. T. Huang, "Reconfigurable monopolar patch antenna," *Electron. Lett.*, vol. 46, pp. 199–200, 2010.

[5] H. F. Abutarboush, R. Nilavalan, S. W. Cheung, and K. Nasr, "Compact printed multiband antenna with independent setting suitable for fixed and reconfigurable wireless communication systems," *IEEE Trans. Antennas Propag.*, vol. 60, no. 8, pp. 3867–3874, Aug. 2012.

[6] H. F. AbuTarboush, R. Nilavalan, K. M. Nasr, S. W. Cheung, T. Peter, and D. Budimir, "Reconfigurable tri-band H-shaped antenna with frequency selectivity feature for compact wireless communication systems," *Microw., Antennas Propag.*, vol. 5, no. 14, pp. 1675–1682, 2011.

[7] V. A. Nguyen, R. A. Bhatti, and S. O. Park, "A simple PIFA-based tunable internal antenna for personal communication handsets," *IEEE Antennas Wireless Propag. Lett.*, vol. 7, pp. 130–133, 2008.

[8] S. K. Oh, Y. S. Shin, and S. O. Park, "A novel PIFA type varactor tunable antenna with U-shaped slot," in *Proc. Int. Symp. Antennas, Propag. EM Theory*, Guilin, China, 2006, pp. 1–3.

[9] Z. J. Jin, J. H. Lim, and T. Y. Yun, "Frequency reconfigurable multiple-input multiple-output antenna with high isolation," *Microw., Antennas Propag.*, vol. 6, no. 10, pp. 1095–1101, 2012.

[10] C. Icheln, "Methods for measuring RF radiation properties of small antennas," Ph.D. dissertation, Dept. Elect. Commun. Eng., Helsinki Univ. Technol., Espoo, Finland, Nov. 2001.

[11] L. Liu, S. W. Cheung, Y. F. Weng, and T. I. Yuk, "Cable effects on measuring small planar UWB monopole antennas," in *Ultra Wideband—Current Status and Future Trends*, M. A. Matin, Ed. New York, NY, USA: InTech, 2012.